

# UC Irvine

## UC Irvine Previously Published Works

### Title

Constraining water table depth simulations in a land surface model using estimated baseflow

### Permalink

<https://escholarship.org/uc/item/91z4p5wv>

### Journal

Advances in Water Resources, 31(12)

### ISSN

0309-1708

### Authors

Lo, Min-Hui  
Yeh, Pat J-F  
Famiglietti, JS

### Publication Date

2008-12-01

### DOI

10.1016/j.advwatres.2008.06.007

### Copyright Information

This work is made available under the terms of a Creative Commons Attribution License, available at <https://creativecommons.org/licenses/by/4.0/>

Peer reviewed



# Constraining water table depth simulations in a land surface model using estimated baseflow

Min-Hui Lo, Pat J.-F. Yeh<sup>1</sup>, J.S. Famiglietti<sup>\*</sup>

Department of Earth System Science, University of California, Irvine, CA 92697, USA

## ARTICLE INFO

### Article history:

Received 11 January 2008

Received in revised form 13 April 2008

Accepted 9 June 2008

Available online 4 July 2008

### Keywords:

Parameter interactions

Calibration

Equifinality

Groundwater model

Baseflow calibration

CLM

Coupled model

## ABSTRACT

Several recent studies have shown the significance of representing groundwater in land surface hydrologic simulations. However, optimal methods for model parameter calibration in order to realistically simulate baseflow and groundwater depth have received little attention. Most studies still use globally constant groundwater parameters due to the lack of available datasets for calibration. Moreover, when models are calibrated, various parameter combinations are found to exhibit equifinality in simulated total runoff due to model parameter interactions. In this study, a simple lumped groundwater model is incorporated into the Community Land Model (CLM), in which the water table is interactively coupled to soil moisture through the groundwater recharge fluxes. The coupled model (CLMGW) is successfully validated in Illinois using a 22-year (1984–2005) monthly observational dataset. Baseflow estimates from the digital recursive filter technique are used to calibrate the CLMGW parameters. The advantage obtained from incorporating baseflow calibration in addition to traditional calibration based on measured streamflow alone is demonstrated by a Monte Carlo-type simulation analysis. Using the optimal parameter sets identified from baseflow calibration, flow partitioning and water table depth simulations using CLMGW are improved, and the equifinality problem is alleviated. For other regions that lack observations of water table depth, the baseflow calibration approach can be used to enhance parameter estimation and constrain water table depth simulations.

© 2008 Elsevier Ltd. All rights reserved.

## 1. Introduction

Numerous modeling studies [18–20,26,29,30,34,36,40,41,47,57,64,65,67] have shown the importance of representing groundwater and soil moisture–groundwater interactions in land surface hydrologic simulations. Most of these studies found that including groundwater can enhance the simulation of evapotranspiration due to the additional moisture provided by the aquifer, while model runoff can be better simulated due to an improved representation of soil moisture. However, optimal methods for model parameter calibration in order to realistically simulate baseflow and groundwater depth have received little attention. Issues regarding how to best specify groundwater parameters remain unclear. Several model intercomparison studies (e.g. [12,50,60]) have shown that with the same atmospheric forcing, the same amount of runoff, but with contrasting baseflow and surface runoff compositions can be simulated. This deficiency leads to varying partitioning between runoff and soil water storage and different responses

in evapotranspiration among different models. Proper modeling of the flow partitioning between surface runoff and baseflow is crucial to the simulation of land surface–atmosphere interactions [35].

It has been well recognized in small-scale watershed modeling studies that various parameter combinations can exhibit “equifinality” in total runoff simulations due to parameter interactions (e.g. [7,8,15,53,54,62]). Different parameter sets can simulate equally acceptable runoff given the constraints from input precipitation and observed streamflow. However, the partitioning between various runoff components can be rather different, especially when only one single target, typically streamflow, is used for calibration [21]. Gallart et al. [24] have shown that the range of acceptable parameter space can be rather wide if the model is calibrated by total runoff alone, while the uncertainty of the subsurface components in the model is large. Nevertheless, parameter uncertainties can be reduced through the use of auxiliary calibration data sets [52] and a multi-criteria calibration framework (e.g. [28,32,62]). Gallart et al. [24] have also used baseflow data and water table records to reduce the uncertainty of baseflow simulations. Moreover, a number of recession curves were used to calibrate the subsurface storage parameters in TOPMODEL (e.g. [5,6,27,49]). Since baseflow is maintained by groundwater discharge, baseflow can be used to determine aquifer parameters [58]. Yu and Schwartz [68] and Gassman et al. [25] have indicated that baseflow separation can provide extra

<sup>\*</sup> Corresponding author. Tel.: +1 949 824 9434; fax: +1 949 824 3874.

E-mail addresses: [mlo@uci.edu](mailto:mlo@uci.edu) (M.-H. Lo), [patyeh@rainbow.iis.u-tokyo.ac.jp](mailto:patyeh@rainbow.iis.u-tokyo.ac.jp) (P.J.-F. Yeh), [jfamigli@uci.edu](mailto:jfamigli@uci.edu) (J.S. Famiglietti).

<sup>1</sup> Present address: Institute of Industrial Science, University of Tokyo, Tokyo 153-8505, Japan.

information for model calibration. Srinivasan and Arnold [56] and Lim et al. [37] have suggested that surface runoff and baseflow should be calibrated individually, because they are usually simulated separately in models and have different sets of parameters for the different generation mechanisms.

However, the concept of distinguishing runoff components in calibration has seldom been applied to land surface models. Most land surface models with groundwater parameterizations assume globally constant parameters related to runoff generation. The primary reason for this simplification is the lack of suitable observations to calibrate these parameters. The disadvantage of specifying globally constant groundwater parameters is critical, e.g., the simulated baseflow and water table depth can not be easily evaluated.

In this study, we demonstrate that the use of baseflow estimates for calibration of relevant model parameters can improve simulations of water table depth and runoff partitioning. It has been widely shown [18–20,47,64] that water table depth can affect the soil moisture profile and land surface hydrologic fluxes. Therefore, albeit that total runoff simulation may be satisfactory, the traditional calibration strategy of using only streamflow may result in a poor simulation of water table depth, soil moisture, and evapotranspiration. In this study, the feasibility of using daily streamflow records and a baseflow separation technique in model calibration is demonstrated using a comprehensive 22-year (1984–2005) hydrologic data set from Illinois. The advantage obtained from incorporating baseflow calibration in addition to traditional calibration based on measured streamflow alone is investigated. The model used in this study is the CLM (Community Land Model) [9,14,48] with a simple lumped groundwater model developed

previously by Yeh and Eltahir [64,65]. The couple model is referred to here as CLMGW.

In Section 2 the CLMGW model, the forcing and calibration data, and the baseflow separation approach used in this study (i.e., the digital recursive filter) are briefly introduced. Section 3 focuses on the sensitivity of CLMGW output to changes in model parameters. The improvement in CLMGW simulations obtained from including baseflow in the model calibration are presented in Section 4. Section 5 summarizes the conclusions and future directions.

## 2. Model and data

### 2.1. Community land model (CLM)

In this study, we incorporate a lumped unconfined aquifer model previously developed by Yeh and Eltahir [64,65] into the CLM, in which the water table is interactively coupled to the soil column through the soil drainage (groundwater recharge) fluxes (see Fig. 1a for a schematic illustration). We use CLM version 3.0, with SIMTOP (simple TOPMODEL-based) runoff [45] and modified frozen soil [46] schemes. In the default CLM, there are 10 soil layers with increasing thickness from 0 to 3.43 m below the surface, and the lower boundary condition at the bottom of the lowest soil layer is universally prescribed as the gravity drainage flux (drainage is equal to the unsaturated hydraulic conductivity).

The surface runoff scheme in the SIMTOP CLM represents both saturation-excess and infiltration-excess runoff as described by the following [45,48]:

$$R_S = F_{\max} e^{-czf} Q_{\text{in}} + (1 - F_{\max} e^{-czf}) \max(0, Q_{\text{in}} - I_{\max}), \quad (1)$$

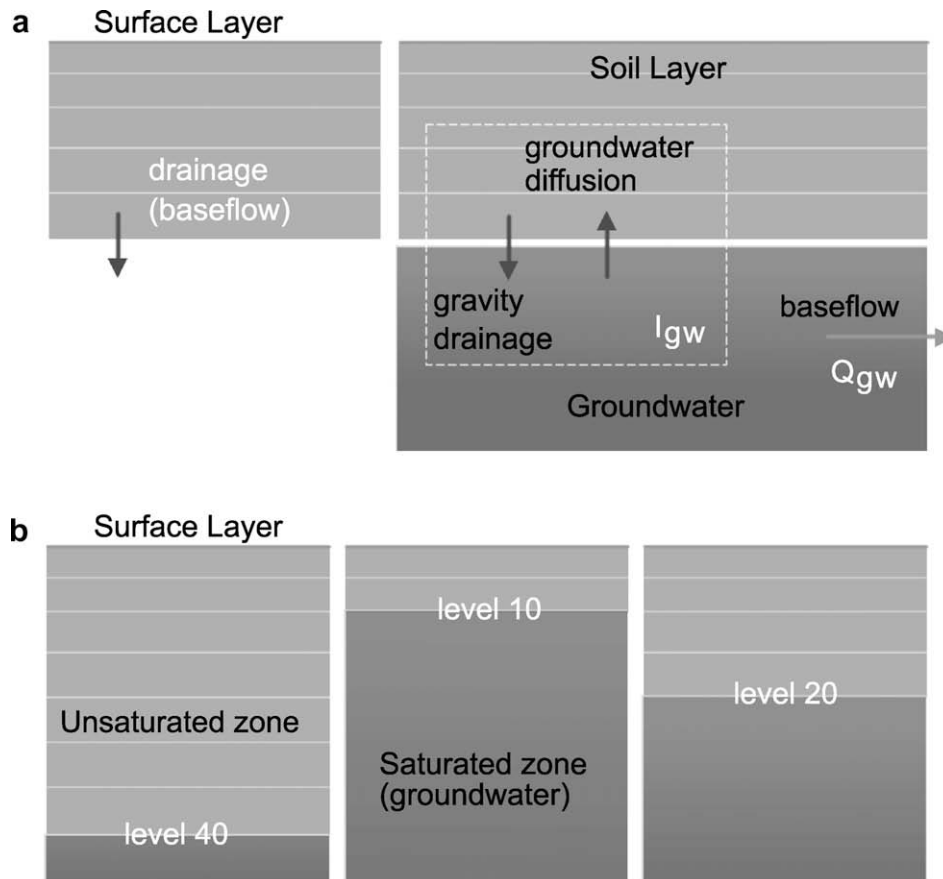


**Fig. 1.** (a) Schematic representation of the soil layer and groundwater model. The left panel is the default CLM without the groundwater model.  $I_{gw}$  is groundwater recharge;  $Q_{gw}$  is groundwater discharge. (b) The flexible soil-layer configuration in the CLMGW structure.

where  $R_s$  [L/T] is the surface runoff,  $F_{max}$  [ ] is the maximum saturated fraction for a grid cell and was set to 0.3 in this study following the default CLM 2.0,  $c$  [ ] is a coefficient for fitting an exponential function to the cumulative distribution function of the topographic index ( $c = 0.5$  as suggested by Niu et al. [45]),  $z$  [L] is the water table depth,  $f$  [L/T] is the soil decay factor (i.e., the length scale for the exponential decrease of the saturated hydraulic conductivity with depth),  $Q_{in}$  [L/T] is the effective precipitation, and  $I_{max}$  [L/T] is the soil infiltration capacity. The first term in Eq. (1) represents saturation-excess runoff, while the second term represents infiltration-excess runoff.

2.2. A lumped groundwater model

A lumped water balance equation for an unconfined groundwater aquifer can be written as [64]

$$S_y \frac{dH}{dt} = I_{gw} - Q_{gw}, \tag{2}$$

where  $S_y$  [ ] is the specific yield of the unconfined aquifer,  $H$  [L] is the groundwater level above a datum,  $I_{gw}$  [L/T] is groundwater recharge, which is the flux at the interface between the unsaturated and saturated zone, i.e., the water table, and  $Q_{gw}$  [L/T] is groundwater discharge to streams (i.e., groundwater runoff).

Groundwater runoff (baseflow)  $Q_{gw}$  at the local scale is formulated using the following threshold relation [65]:

$$\begin{aligned} Q_{gw} &= K(d_0 - d_{gw}) & \text{if } 0 \leq d_{gw} \leq d_0, \\ Q_{gw} &= 0 & \text{if } d_{gw} \geq d_0, \end{aligned} \tag{3}$$

where  $K$  [1/T] is the outflow constant inversely proportional to the aquifer residence time,  $d_0$  [L] is the threshold depth at which groundwater runoff is initialized, and  $d_{gw}$  [L] is the water table depth (always positive). When applying Eq. (3) to a grid cell in a climate model, the grid-scale groundwater runoff ( $Q_{gw}$ ) cannot be determined solely from the grid-mean water table depth ( $d_{gw}$ ) because of the nonlinear relationship between them. Yeh and Eltahir [65] proposed a statistical–dynamical approach to account for the influence of the subgrid heterogeneity of water table depth on the grid scale  $Q_{gw}$ . The grid-scale groundwater runoff accounting for subgrid heterogeneity of the water table depth can be derived as [65, Eq. (5)]

$$\begin{aligned} E[Q_{gw}] &= \frac{K\lambda^\alpha}{\Gamma(\alpha)} \left\{ d_0 \left[ \frac{(\alpha - 1)!}{\lambda^\alpha} - e^{-\lambda d_0} \sum_{k=0}^{\alpha-1} \frac{(\alpha - 1)!}{k!} \frac{d_0^k}{\lambda^{\alpha-k}} \right] \right. \\ &\quad \left. - \left[ \frac{\alpha!}{\lambda^{\alpha+1}} - e^{-\lambda d_0} \sum_{k=0}^{\alpha} \frac{\alpha!}{k!} \frac{d_0^k}{\lambda^{\alpha-k+1}} \right] \right\}, \end{aligned} \tag{4}$$

where  $E[Q_{gw}]$  is the grid-scale groundwater runoff,  $\Gamma(\alpha)$  is the gamma function,  $\alpha$  and  $\lambda$  are the shape and scale parameter of the assumed Gamma distribution of water table depth, respectively. In the groundwater model (Eqs. (2) and (4)), there are in total four parameters:  $d_0$ ,  $K$ ,  $S_y$ , and  $\alpha$ .

The groundwater model in Eq. (2) is interactively coupled with the soil model in the CLM. In this work we use a total of 50 soil layers: from the first to fifth soil layer (0–20cm), the layer thicknesses are the same as the default thicknesses in the CLM, i.e., from the first to fifth layer, the soil layer thicknesses are 1.75, 2.76, 4.55, 7.50, and 12.36 cm, respectively. Below the fifth layer, the layer thickness is a constant 20 cm from 0.2 m to 9.2 m deep. The soil model and groundwater model are decoupled when the water table falls below 9.2 m. The total length of the active unsaturated soil column varies in response to water table depth fluctuations by keeping the number of unsaturated layers variable (see Fig. 1b).

2.3. Data

Soil moisture data were collected by the Illinois State Water Survey (ISWS) from 1981 through the present at 19 stations using neutron probes. Weekly to biweekly measurements of soil wetness were taken at 11 different soil layers with a resolution of about 20 cm down to 2 m below the surface [31], and no data were collected below 2 m. Fifteen of these 19 sites covering a 22-year simulation period (1984–2005) are used in this study. The data on water table depth consists of 19 groundwater wells scattered throughout Illinois which are used to monitor the unconfined silt loam aquifers. These aquifers are relatively shallow and the average depth to the water table ranges between 1 and 10 m below the surface. Ten out of 19 wells with complete monthly records from 1984 to 2005 are used in this study. Streamflow data collected by the US Geological Survey consists of daily discharge measurements at the outlets of three largest basins in Illinois: Illinois River, Rock River, and Kaskaskia River. Their total drainage areas cover approximately two thirds of the area of Illinois. Their respective 22-year (1984–2005) monthly discharge is weighted by the drainage area to give an estimate of average streamflow in Illinois. Fig. 2 shows the locations of the data sampling networks in Illinois; for other details on the Illinois hydrologic data, the readers are referred to Yeh et al. [63].

To drive the CLMGW in an offline simulation, six input atmospheric forcings are required: precipitation, solar radiation, near surface air temperature, air humidity, air pressure, and wind speed. Precipitation and temperature are taken from the National Climate Data Center (NCDC, <http://www.ncdc.noaa.gov/oa/ncdc.html>) Integrated Surface Hourly data set. Seventeen NCDC stations located in Illinois are selected to derive state-average values by simple averaging. Air humidity, pressure, wind speed, and solar radiation are taken from the 6-hourly reanalysis data from National Centers for Environmental Prediction–Department of Energy (NCEP-DOE) [33] and linearly interpolated to a 3-hourly resolution. In addition, the monthly average of solar radiation is bias-corrected for consistency with the NASA Surface Radiation Budget monthly data set. The vegetation type in the CLMGW is specified as 60% corn, 22% broadleaf-deciduous-temperate-tree, 9% C3 grass, and 9% C4 grass, which were derived based on 1 km satellite data and climate rules as described in Bonan et al. [10]. The rooting depth is specified as 1.5 m from a comprehensive global field survey dataset by Zeng [69].

2.4. Baseflow separation

Numerous techniques for hydrograph separation exist in the hydrologic literature [51]. Here we adopt the digital recursive filter technique in order to separate baseflow from daily streamflow records in Illinois. The digital recursive filter technique has gained increasing popularity in recently published hydrologic literature (e.g. [1,2,11,16,44]). These studies have indicated that the digital recursive filter technique is efficient, reproducible, and objective. The digital recursive filter technique was originally used in signal analysis and processing [38], and has been applied to separate baseflow from measured daily streamflow [11,22,23,44]. The digital recursive filter technique has been used in numerous previous studies, and its performance has been considered as satisfactory as traditional hydrograph separation approaches [1,3,39]. Arnold and Allen [2] showed that the digital recursive filter can have a high coefficient of determination (0.86) compared to field measurements. Szilagyi [59] stated that the performance of the digital filter is as good as physically based simulations of baseflow. Moreover, this technique has also been used in automated methods to estimate baseflow and groundwater recharge from streamflow records [2], and for the automated web geographic information system-based hydrograph analysis tools [37].

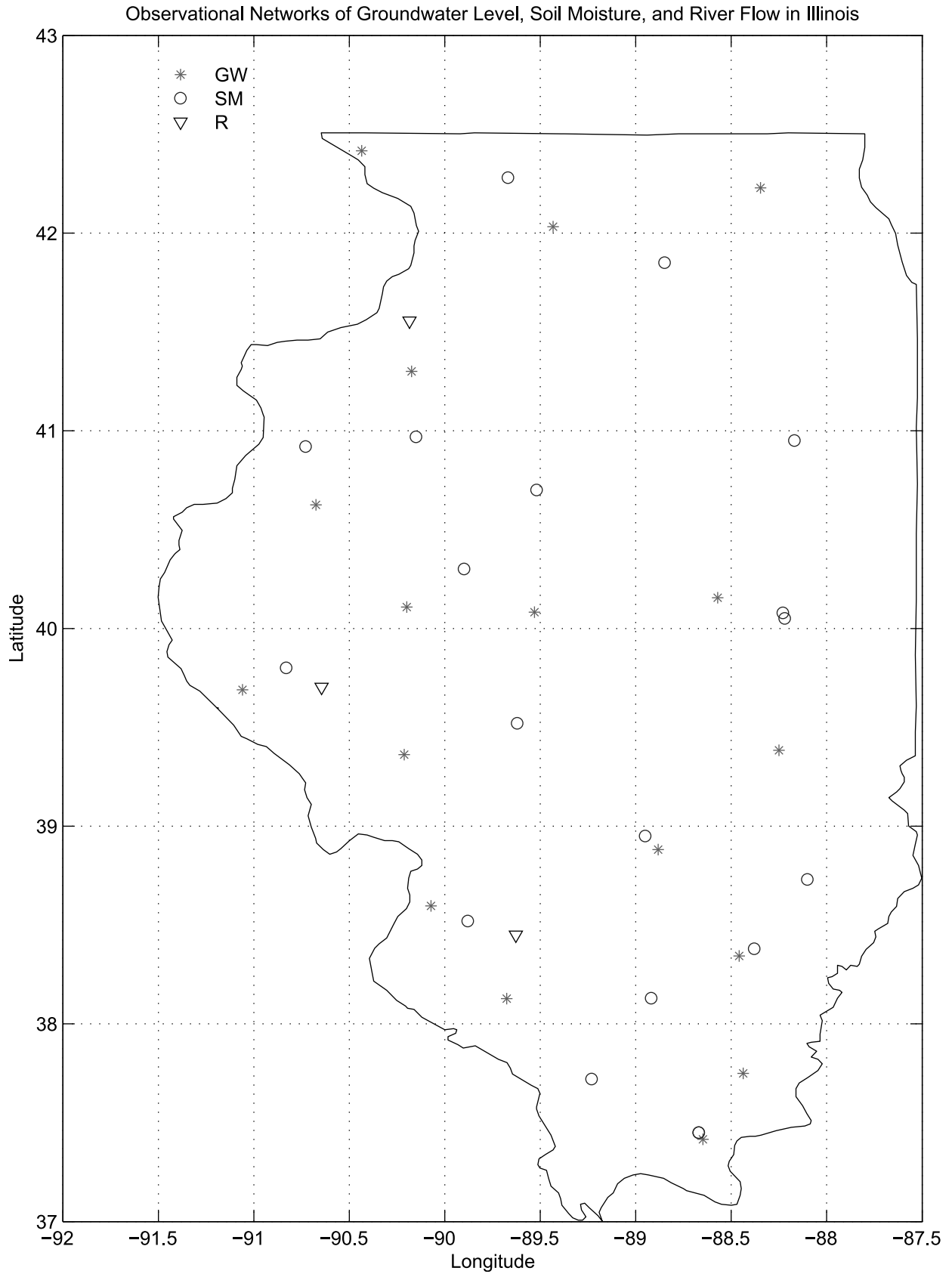


Fig. 2. The locations of the data sampling network of soil moisture (SM), water table depth (GW), and streamflow (R) in Illinois.

According to the digital filter technique, baseflow at time  $t$  can be written as [11]

$$B(t) = aB(t - 1) + 0.5(1 - a)[F(t) + F(t - 1)], \quad (5)$$

where the fast flow component,  $F(t)$ , can be estimated from the total runoff  $Y(t)$ :

$$F(t) = \frac{(3a-1)}{(3-a)}F(t-1) + \frac{2}{(3-a)}[Y(t) - aY(t-1)], \quad (6)$$

where  $a$  is the filter coefficient with a feasible range between 0.9 and 0.975 [1,16,42,44]. Eqs. (5) and (6) represent a low-pass filter; the larger the  $a$  is, the more high frequency components are filtered out. Although the digital filter technique lacks a physical basis, it is more objective and easier to implement than traditional graphical separation techniques. Fig. 3 shows baseflow estimates using various filter coefficient,  $a = 0.900, 0.925, 0.950$  and  $0.975$ . Spongberg [55] indicated that baseflow may also contain certain amounts of high frequency variability; therefore, the digital recursive filter should be used with caution. In this study, we adopt the maximum values of the daily baseflow estimates from using different filter coefficients as shown in Fig. 3 in order to prevent excessive attenuation of the filtered baseflow signals.

Fig. 4 presents a scatter plot of the 22-year (1984–2005) baseflow estimates (from the digital recursive filter) and the observed water table depth at both monthly and daily time scales. Daily water table depth is approximated from linear interpolation of the 22-year monthly water table depth time series. This can be justified given the dominant low-frequency nature of groundwater variability. As shown, a strong correlation exists between these two variables: their correlation coefficient is 0.75 at the monthly

time scale and 0.80 at the daily scale. Based on the same Illinois data set as used here, Eltahir and Yeh [17, Fig. 7b] estimated that groundwater runoff accounts for  $\sim 75\%$  of the streamflow variance in Illinois. Snow and tile drainage processes also play a role in the baseflow contribution to streamflow. Yeh et al. [63] reported that after a day with snowfall in Illinois, snow accumulation typically lasts only through the subsequent 1–5 days. As such they concluded that the snow storage effect is insignificant for monthly water balance in Illinois. Yeh et al. [63] also reported that human withdrawal or interference in streamflow is not significant in the regional water balance of Illinois. In fact it is negligible compared to the other variables in the water balance. Therefore, we assume that snow processes or anthropogenic effects can be neglected in this particular large-scale study.

### 2.5. Model evaluation

To evaluate the ability of the CLMGW to simulate variability of the hydrologic fluxes, the 22-year (1984–2005) monthly time series of model-simulated total runoff, baseflow, groundwater recharge, soil moisture, and water table depth are plotted in Fig. 5 against observations. In this study, the data on total runoff, soil moisture, and water table depth are from in situ measurements. Soil moisture is the weighted average of the 11-layer measurements from 0 to 2 m below the surface, and then spatially-averaged over Illinois. Water table depth is the spatial-average from 10 monitoring wells in

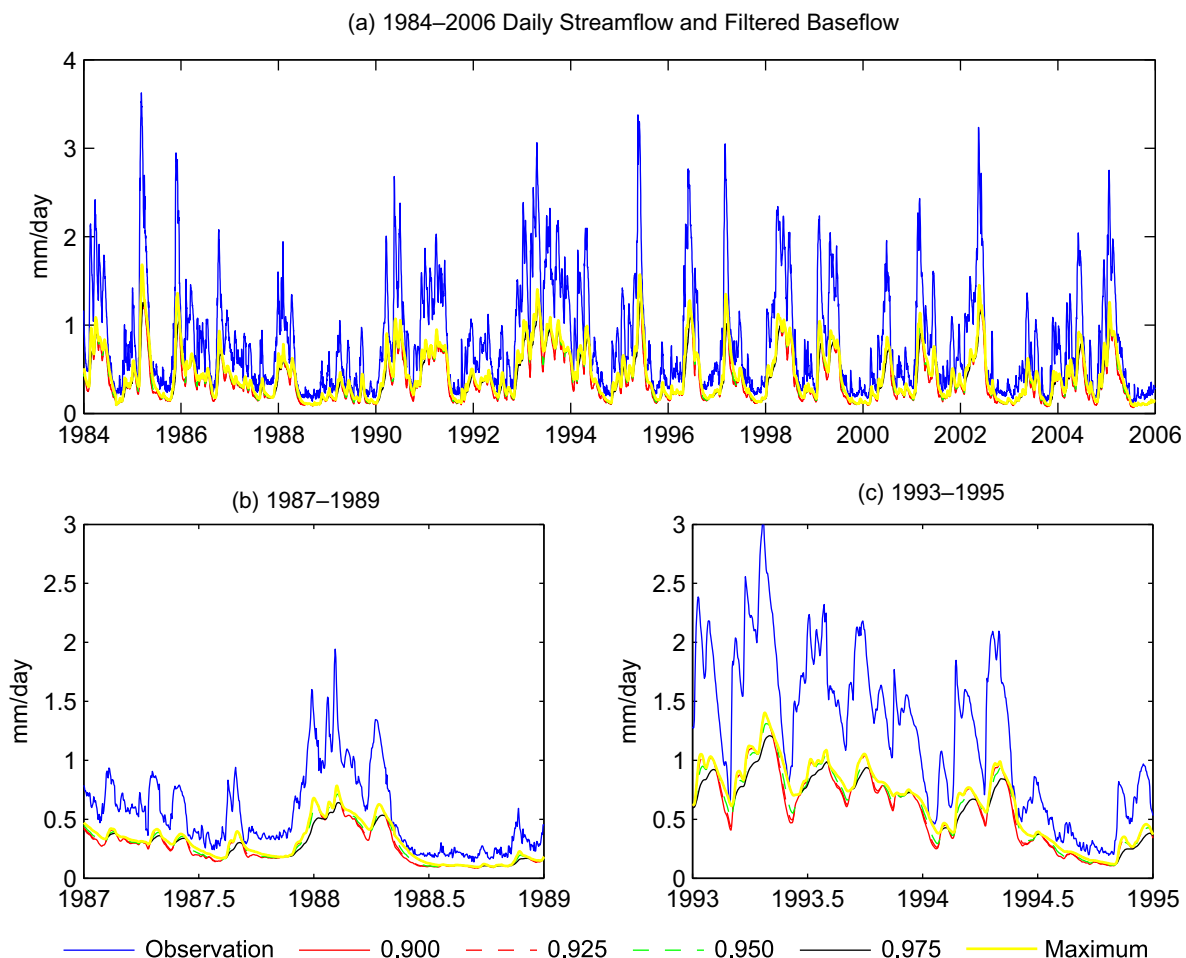
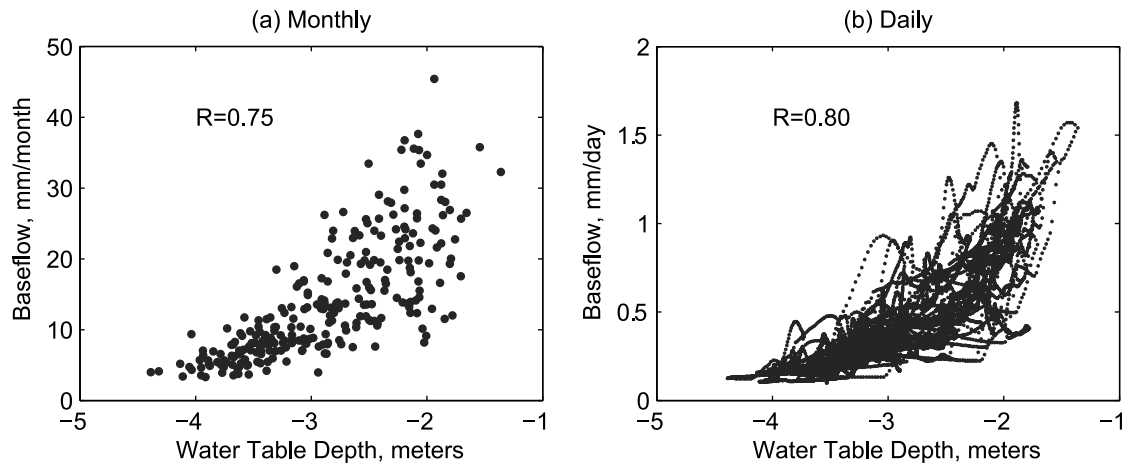


Fig. 3. (a) Baseflow estimates from using various filter coefficient,  $a = 0.900, 0.925, 0.950$ , and  $0.975$ . The bold yellow line is the maximum values of the daily baseflow estimates from using different filter coefficients. (b) and (c) are the same as (a), but the time period are for 1987–1989 and 1993–1995, respectively.



**Fig. 4.** The (a) monthly and (b) daily scatter plots of the 22-year (1984–2005) baseflow estimated from the daily average streamflow records in Illinois using the digital recursive filter versus observed water table depth.

Illinois, each with the complete 22-years (1984–2005) of monthly data. The “observed” baseflow is derived by hydrograph separation using the digital recursive filter, and the “observed” recharge is estimated by soil water balance; for details, see Yeh and Famiglietti [66].

It can be seen from Fig. 5 that in general the CLMGW faithfully reproduces the observed monthly and longer time scale variations of these variables, in particular the anomalously low (high) baseflow, soil moisture and water table depth in drought (flood) conditions during the simulation period (Fig. 5b, d, and e). However, peak flows were often under-simulated (Fig. 5a) by the CLMGW with the most notable cases around 2000–2001 when the simulated water table depth was significantly biased deep (Fig. 5e). Moreover, for groundwater recharge simulations, the CLMGW not only reproduces most of the observed peaks fairly well (such as those that occurred in 1985, 1995, 1996, and 2004), it also reproduces the observed upward groundwater fluxes (i.e., negative recharge) for the most of summer months (Fig. 5c). Negative recharge is an upward capillary flux from the aquifer to replenish root-zone soil moisture, resulting in a decline of water table depth during the dry season. It is an important water source during extended dry periods which can affect the soil moisture vertical profile and feedback to influence predictions of land surface water and energy fluxes. This is attributed to the explicit representation of shallow water table dynamics such that the intimate interaction between the soil moisture and shallow aquifer can be well simulated in the CLMGW.

### 3. Parameter sensitivity

A Monte Carlo-type simulation analysis is adopted here to investigate parameter sensitivity. The parameters in the CLMGW include the baseflow parameters  $d_0$ ,  $K$ ,  $\alpha$ , and  $S_y$  (Eqs. (2) and (4)), soil pore size index  $b$  from the water-retention equation of Clapp and Hornberger [13], and the surface runoff parameters  $c$ ,  $f$ , and  $F_{\max}$  (Eq. (1)). After extensive sensitivity testing with respect to the above parameters, the  $f$ ,  $b$ ,  $d_0$ , and  $K$  parameters were determined to have the largest influence on runoff generation of the CLMGW, and hence they are treated as the calibration parameters in this study. The first parameter is the soil decay factor  $f$ , which originated from the TOPMODEL formulation. The second is the soil pore size index  $b$  which affects soil hydraulic conductivity and water potential. According to Yeh and Eltahir [65], the parameters with the largest influence on the groundwater model (Eqs. (2) and (4)) are  $d_0$  and  $K$ . These two parameters jointly control the water

table dynamics and baseflow generation. Model simulations are found to be relatively insensitive to the remaining two groundwater parameters ( $\alpha$  and  $S_y$ ), and thus they are specified in this study as 4 and 0.08, respectively, as suggested by Yeh and Eltahir [65] for Illinois.

For each of the four parameters, seven uniformly distributed parameter values are determined from their feasible ranges as given in Table 1. The Monte Carlo-type simulation analysis is used here, in which the CLMGW model was run using all the combinations of four parameters, consists of a total of  $7^4$  (=2401) simulations. The simulation and calibration were conducted in Illinois using the 22-year (1984–2005) atmospheric forcing data. In order to ensure that the simulations were independent of uncertain initial conditions, nine spin-up years, all with 1984 forcing, were superimposed before the beginning of the 22-year (1984–2005) simulation, but they were disregarded in the analysis of model results. For shallow water table areas, the number of spin-up years required for the water table to reach equilibrium is usually less than 5 years [47].

Fig. 6 plots the 22-year climatology of simulated total runoff, baseflow, water table depth, and surface runoff. Each of the seven lines in each panel represents the average of  $7^3$  (=343) runs with one of the 4 calibration parameters fixed at a given value. It shows the overall model sensitivity to flow partitioning and water table depth simulation. When  $f$  is low, the surface runoff is high (due to the higher saturated fractional area, see Eq. (1)) and less water infiltrates into the soil resulting in lower baseflow and deeper water table depth (Fig. 6b and c). Baseflow shows almost no seasonal variability for the lowest  $f$  (Fig. 6b) because most of the effective precipitation is lost through surface runoff. As  $f$  increases, baseflow increases and surface runoff decreases (Fig. 6b and d). Due to these compensating effects, the effect of  $f$  on the total runoff becomes more complex: from January to March the higher  $f$  causes higher total runoff, but the trend reverses from April on.

The parameter  $b$  affects soil water potential in that a higher  $b$  causes lower soil water potential and hence lower groundwater recharge, deeper water table depth and less baseflow. However, the effect of  $b$  on the flow partitioning and water table depth simulation is small relative to  $f$  (Fig. 6e–h).

As shown in Eq. (3),  $d_0$  is the threshold depth for baseflow generation at the local scale, while  $K$  is the baseflow rate constant which is inversely proportional to the residence time of the aquifer. The seasonal cycles of baseflow and water table depth show significant sensitivity to both parameters (Fig. 6j, k, n, and o). As  $d_0$  increases, baseflow increases resulting in a lower water table (Fig.

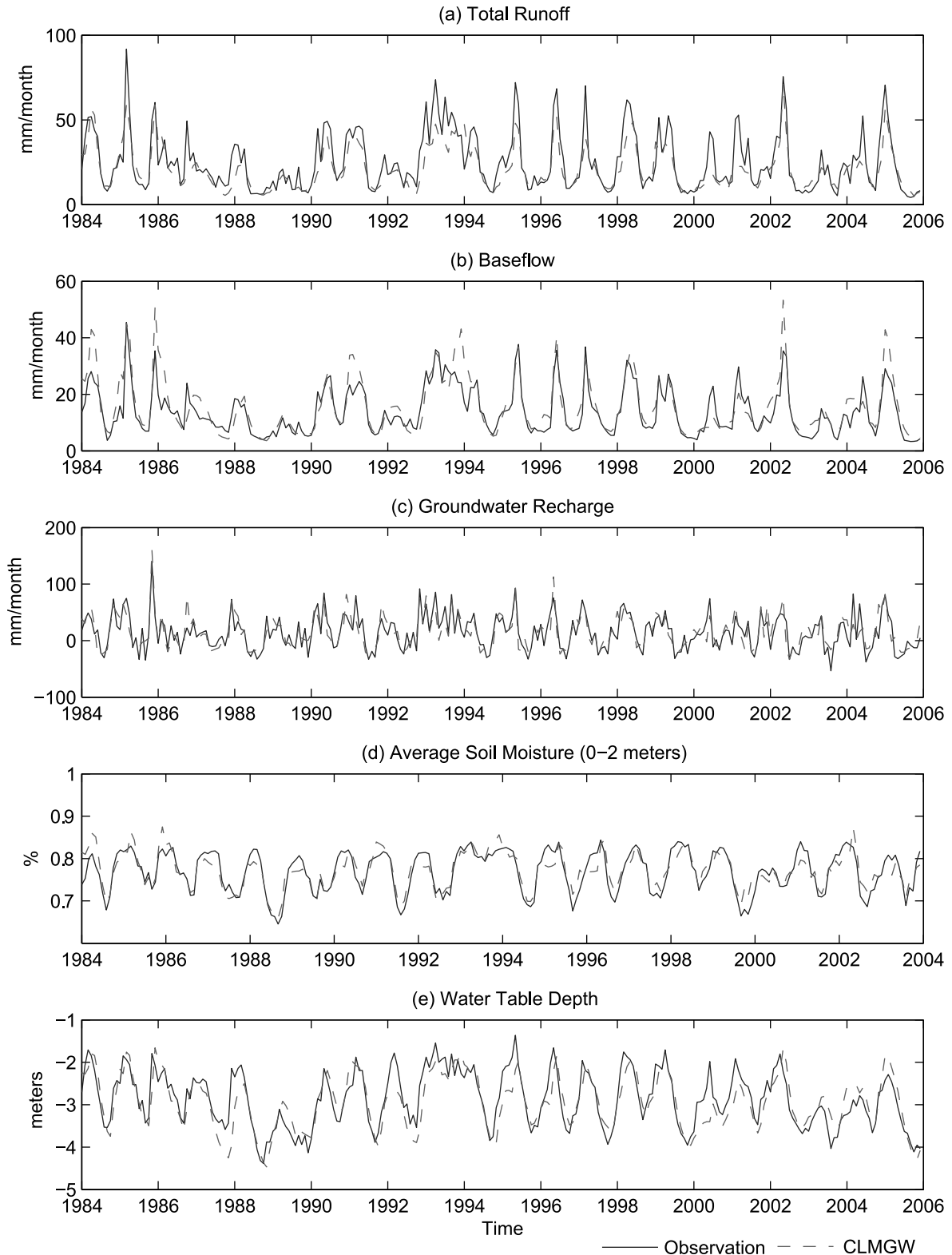


**Fig. 5.** The 22-year (1984–2005) monthly time series of (a) total runoff, (b) baseflow, (c) groundwater recharge, (d) soil moisture, and (e) water table depth in comparison with observations.

6j and k) and lower surface runoff (Fig. 6l) according to the surface runoff scheme of SIMTOP in Eq. (1). The seasonal cycles of baseflow and water table depth become progressively flatter as  $d_0$  increases (Fig. 6j and k), and the mean water table depth becomes deeper and deeper, eventually resulting in the decoupling of the aquifer and

soil moisture. Hence  $d_0$  has a major impact on the seasonal cycles of total runoff (Fig. 6i) with the greatest seasonal variations found in the lowest  $d_0$  range which inhibits the baseflow generation. Concerning the parameter  $K$ , despite its significant impact on the seasonal cycle of both the surface runoff and baseflow (Fig. 6n and

**Table 1**

The ranges of the four calibration parameters in the CLMGW model used in the Monte Carlo analysis

Parameter	Units	Values
Decay factor, $f$	$m^{-1}$	0.05, 0.40, 0.75, 1.10, 1.45, 1.80, 2.15
Clapp and Hornberger, $b$		5, 6, 7, 8, 9, 10, 11
$d_0$	m	0.5, 1.0, 1.5, 2.0, 2.5, 3.0, 3.5
$K$	month <sup>-1</sup>	10, 50, 90, 130, 170, 210, 250

p), its combined impact on total runoff is negligible (Fig. 6m). The  $K$  parameter has a more moderate influence on baseflow than  $d_0$ : it primarily controls the residence time of groundwater reservoir and hence the rate of baseflow generation and the equilibrium position of water table depth. A larger  $K$  represents a more efficient groundwater dissipation mechanism leading to a larger baseflow rate and hence deeper equilibrium water table depth.

Fig. 7 shows the 22-year average annual total runoff, baseflow, and surface runoff. Each curve represents the average from the 343 runs in all of which only one of the four parameters are fixed. As seen from Fig. 7a, although the amount of total runoff is insensitive to the  $f$  value, the partitioning between surface runoff and baseflow is remarkably sensitive to the  $f$ . This suggests equifinality in an optimal parameter set: i.e., that an optimal parameter set calibrated against observed total streamflow does not lead to a unique

and correct flow partitioning. It also implies that if only one criterion is used in the parameter calibration, then model simulations for other hydrologic variables may not be constrained. Moreover, other than  $f$ , the parameter  $d_0$  also has significant impact on the flow partitioning (Fig. 7c). In contrast, the parameters  $b$  and  $K$  have a relatively lower impact on the flow partitioning (Fig. 7b and d). The  $K$  parameter loses most of its impact as  $K$  increases. Although the flow partitioning simulations show little sensitivity to  $b$ , it significantly changes patterns of groundwater recharge, baseflow, and water table depth simulations (not shown) by affecting the rate of soil water fluxes in the soil column through Richards equation.

These four calibration parameters have combined influences on either the total runoff partitioning or simulations of other hydrologic variables. To summarize: (1)  $f$  determines to a large extent the flow partitioning between surface runoff and baseflow; (2)  $b$  affects the pattern of groundwater recharge; (3)  $d_0$  significantly affects the amount of baseflow generation and the long-term average water table depth, which further indirectly affects the amount of surface runoff generated; (4)  $K$  primarily affects the timing of baseflow generation rather than the amount (which is primarily controlled by the  $d_0$ ). Therefore, only by calibrating these relevant parameters with respect to surface runoff or baseflow can the problem of equifinality be avoided and the correct flow partitioning be achieved. In the following section, the improvement

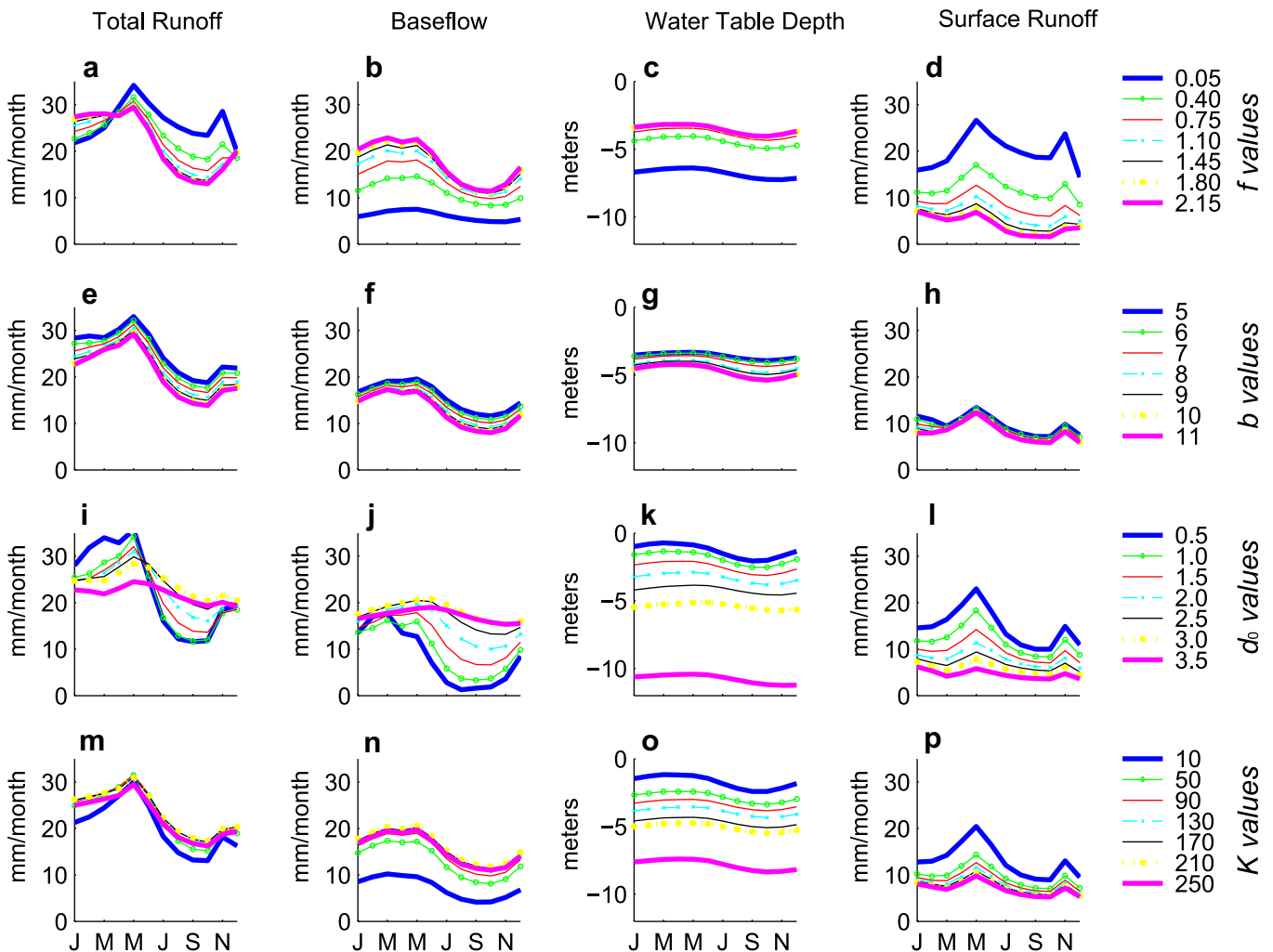


**Fig. 6.** The 22-year climatology of the simulated total runoff, baseflow, water table depth, and surface runoff. Each of the seven lines in each panel represents the average of 7<sup>3</sup> (=343) runs with one of the four calibration parameters fixed at the given value.

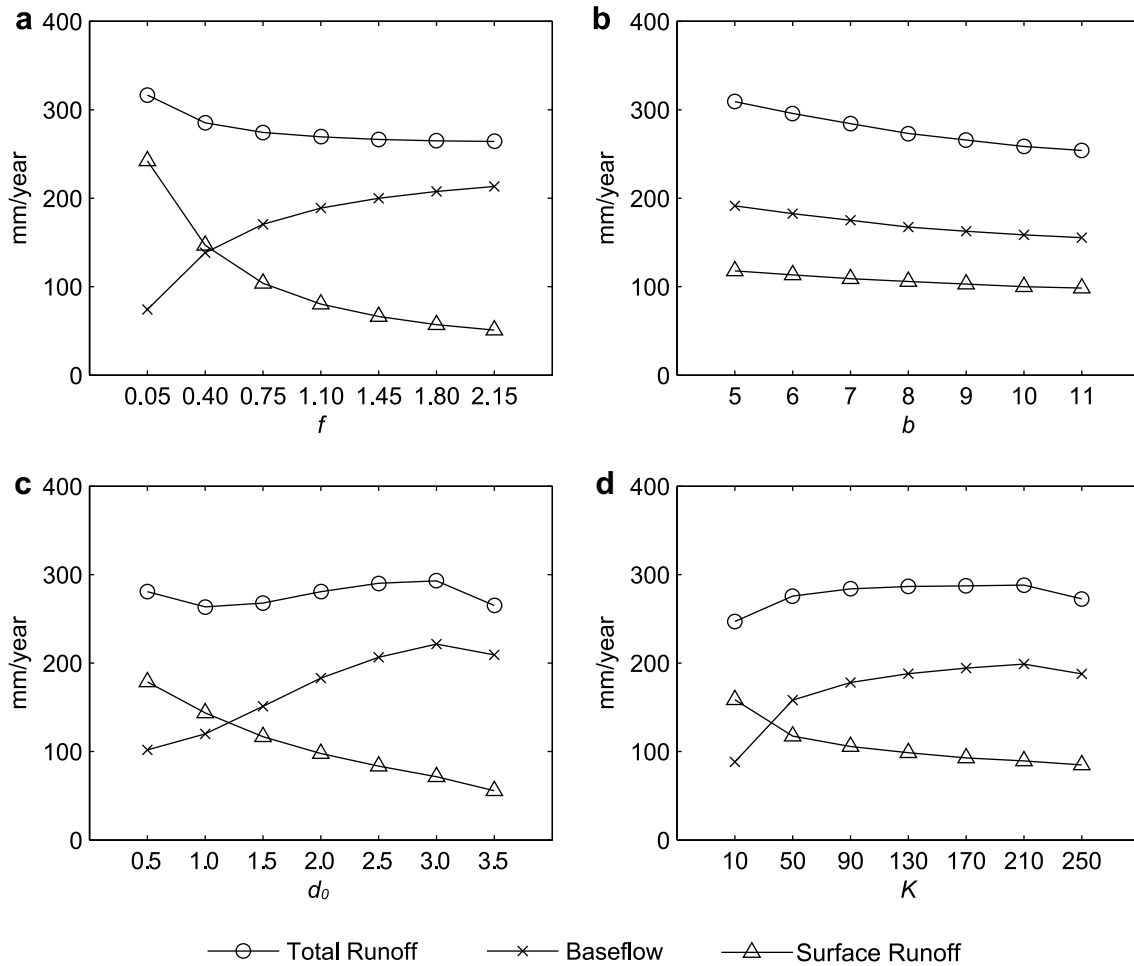


Fig. 7. The average annual amounts of total runoff, baseflow, and surface runoff. Each curve represents the average from the 343 runs with only one of the four parameters ( $f, b, d_0$ , and  $K$ ) fixed.

obtained from utilizing baseflow information in CLMGW parameter calibration will be demonstrated.

#### 4. Improving water table depth simulations by baseflow calibration

The Nash–Sutcliffe coefficient of efficiency (N-S) [43] is used here as the statistical criterion for the evaluation of model simulation of total runoff, baseflow, and water table depth:

$$NS = 1 - \frac{\sum_{i=1}^n (o_i - p_i)^2}{\sum_{i=1}^n (o_i - \bar{o})^2}, \quad (7)$$

where  $o$  is the observation,  $p$  is the model estimate,  $\bar{o}$  is the mean of the observation. The N-S coefficient measures the overall goodness of fit between the observations and model simulations. For a perfect simulation, the N-S coefficient is equal to one. We also tested the RMSE (root-mean-square error) as an alternative statistical measure of model performance, and found similar results to the N-S coefficient. Thus, only the N-S coefficient is used to evaluate model performance for the remainder of this study.

All 2401 runs are ranked according to the N-S coefficient of their total runoff simulation. Fig. 8a presents the N-S coefficients of total runoff, baseflow, and water table depth simulations for the top-scoring 1% of total runoff calibration runs. As expected, these 24 runs all have high N-S coefficients for total runoff simulations, but the same cannot be said for the baseflow and water table depth

simulations. As previously shown in Fig. 6, variations in the calibration parameters have a larger impact on flow partitioning than the total runoff simulation. The major reason is that the total runoff simulation is to a large extent being constrained by the precipitation forcing and evapotranspiration simulation; however, the simulation of runoff components (surface runoff and baseflow) depends closely on the relevant parameter values calibrated. Therefore, additional calibration targets may be required to constrain the baseflow and water table depth simulations of the model.

Here we propose to use the baseflow estimates as an alternative calibration target in addition to the traditional calibration using only streamflow. Due to the strong correlation shown in Fig. 4, we expect that the advantage obtained from incorporating baseflow calibration in constraining water table depth simulations can be demonstrated. Fig. 8b presents the comparison of the N-S coefficients of the water table depth simulation between the top-scoring 1% runs calibrated, respectively, from the total runoff and from the estimated (filtered) daily baseflow. Note that in Fig. 8b the parameter sets of each run for the two calibration targets are different; therefore it cannot be compared point by point. Fig. 8b clearly shows that the baseflow calibration runs with the top-scoring 1% in general have a higher N-S coefficient for water table depth simulations than that of the top-scoring 1% total runoff calibration runs. In addition, most of the simulated water table depths from the top-scoring 1% of baseflow calibration runs are within the top-scoring 20% of the water table depth simulations, and their baseflow ratio is closer to the observed value (~0.6). These results

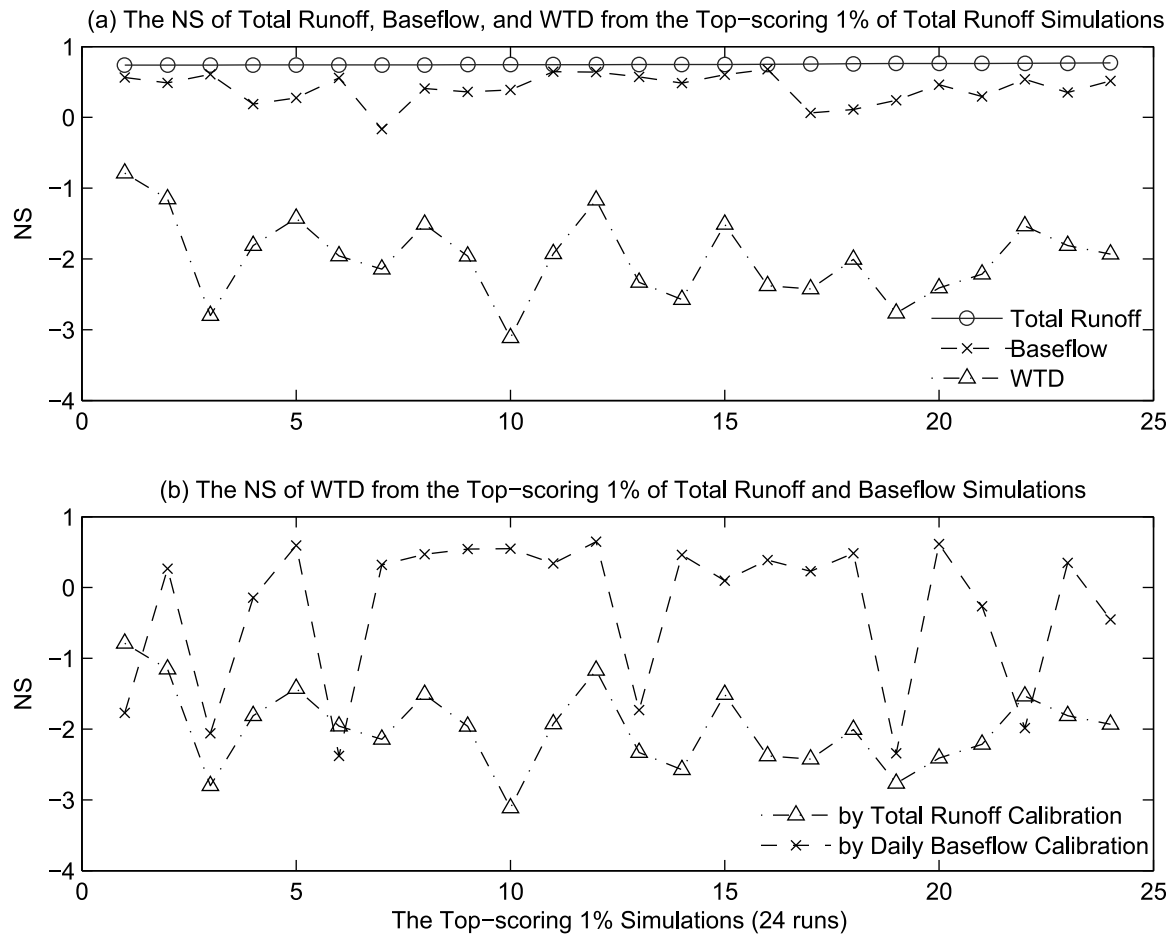


**Fig. 8.** (a) The NS coefficient for the top-scoring 1% (24 runs) of total runoff, baseflow, and water table depth simulations, (b) the NS coefficient comparison of the simulated water table depth between the top-scoring 1% runs calibrated against the total runoff and (filtered) daily baseflow data.

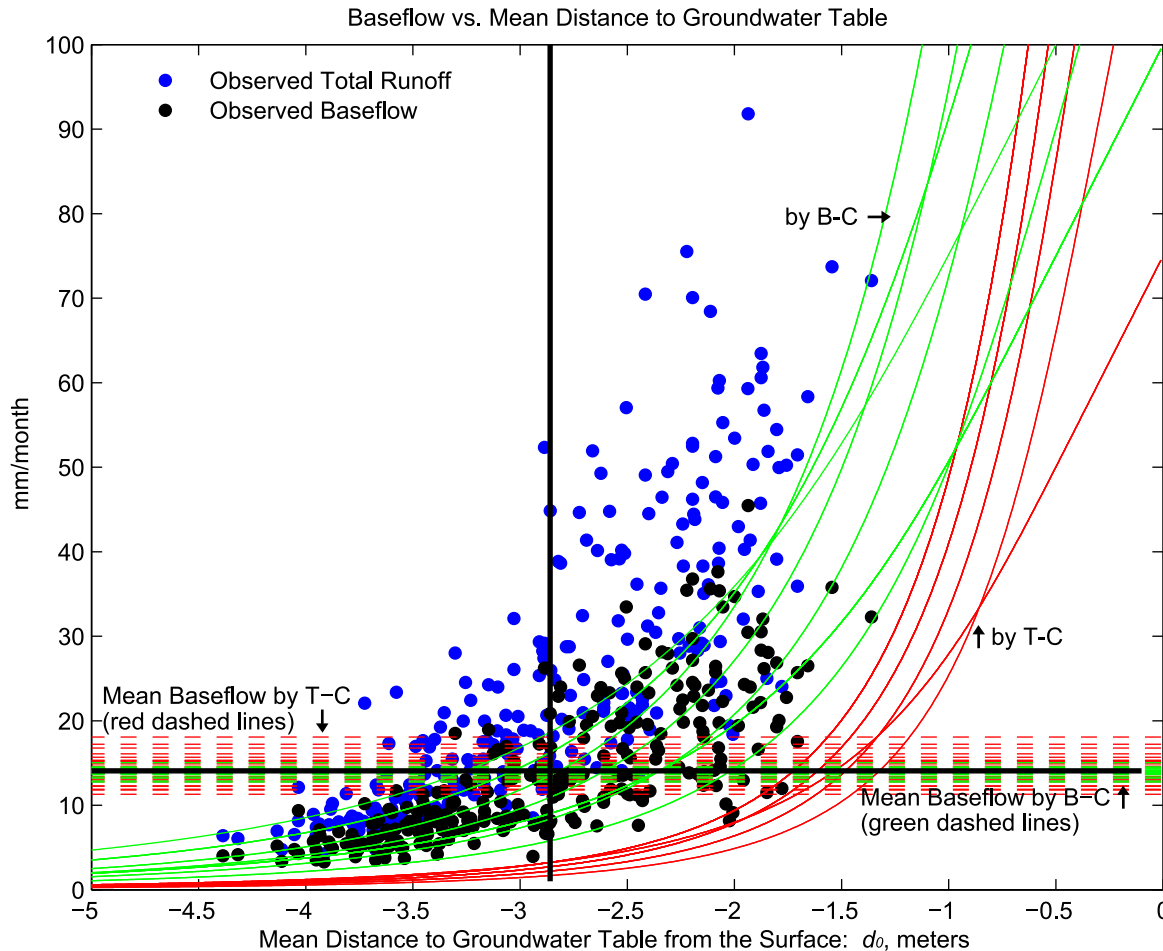
demonstrate the benefit of using baseflow calibration to constrain model simulations of water table depth.

Fig. 9 plots two groups of groundwater rating curves (i.e., the average baseflow  $Q_{gw}$  versus the average water table depth  $d_{gw}$ ) calibrated from the top-scoring 1% runs of the baseflow and total runoff simulations, respectively, compared with the observed (state-average) groundwater rating curve. The groundwater rating curve controls the relationship between the water table depth and baseflow. The group of green rating curves is plotted from Eq. (4) with various combinations of  $d_0$  and  $K$  calibrated from the filtered daily baseflow, while the red curves are calibrated from the observed streamflow. The two bold black lines indicate the mean observed water table depth ( $-2.86$  m) and the mean filtered baseflow rate ( $\sim 14$  mm/month). Note that there are six points from the baseflow calibration with low performance of water table depth simulations excluded in this figure. Blue dots are the observed total streamflow versus observed water table depth, and black dots are the baseflow obtained from the filter technique versus the observed water table depth. The differences between the blue and black dots can be regarded as the surface runoff estimation. As clearly shown, there are two distinct groups of calibrated groundwater rating curves: the green rating curves cross the observed data whereas the red curves are located outside the observed data.

The horizontal red and green dashed lines mark the mean baseflow rates for the top-scoring 1% runs of the total runoff and the baseflow calibrations, respectively. As seen from Fig. 9, the mean baseflow rates simulated from the total runoff calibration (red

lines) have a wider range compared to those simulated from the baseflow calibration (green lines). The intersection between the horizontal lines (mean baseflow rate) and the groundwater rating curves in Fig. 9 gives the average water table depth. As seen, the mean water table depths show distinct differences: the average water tables from the baseflow calibration are on average 1–1.5 m deeper than those from the total runoff calibration, and they are closer to the observed average water table depth of 2.86 m. It can be observed from Fig. 8a that the water table depth simulated from the total runoff calibration are not correct as a result of the incorrect rating curve identified. Owing to its strong dependence on baseflow as shown in Fig. 4, the water table dynamics can be simulated more accurately by calibration using baseflow data.

Table 2 summarizes the 22-year average annual total runoff, surface runoff, baseflow, and water table depth from the top-scoring 1% runs from the total runoff and baseflow calibrations in comparison with the corresponding observed values. As shown, the total runoff simulated from both calibration approaches are underestimated especially for the surface runoff simulation. One possible reason for this bias is that in this study we used average atmospheric data as the input forcing. The averaging process has smoothed out the temporal intensity and the spatial variability of precipitation such that surface runoff is underestimated. Moreover, although there is not much difference in the mean baseflow between the two cases, the water table depth simulated from the case of the total runoff calibration is biased shallow due to the incorrect groundwater rating curve identified.



**Fig. 9.** Two groups of groundwater rating curves (i.e., the average groundwater runoff,  $Q_{gw}$ , versus the average water table depth,  $d_{gw}$ ) calibrated from the top-scoring 1% runs of the baseflow and total runoff simulations, respectively, in comparison with the observed state-average groundwater rating curve. The group of green rating curves is plotted by Eq. (4) with different combinations of  $d_0$  and  $K$  calibrated from the filtered daily baseflow data, while the red curves were calibrated from total streamflow measurements. The horizontal red and green dashed lines mark the mean baseflow rate for the top-scoring 1% runs of the total runoff and baseflow calibrations, respectively. The two bold black lines indicate the mean water table depth ( $-2.86$  m) and the mean filtered baseflow rate ( $14.07$  mm/month). T-C indicates total runoff calibration; B-C indicates baseflow calibration.

**Table 2**

The 22-year average annual total runoff, surface runoff, baseflow, and water table depth from the top-scoring 1% runs from the total runoff and the baseflow calibrations in comparison with the corresponding observed values

Variables	Total runoff calibration	Baseflow calibration	Observation
Total runoff, mm/year	279.5	266.6	301.0
Surface runoff, mm/year	108.4	99.9	132.1
Baseflow, mm/year	171.1	166.7	168.9
Water table depth, m	$-1.79$	$-2.76$	$-2.86$

## 5. Discussion and conclusions

Although several recent land surface modeling studies have shown the importance of water table dynamics and various groundwater parameterizations have been developed, the problem regarding how to best specify groundwater parameters in order to realistically simulate baseflow and groundwater depth has received little attention. Most of these previous studies assume globally constant parameters due to the lack of data sets characterizing large-scale groundwater variability. Here we test the hypothesis that the use of the baseflow information contained in streamflow

data in model calibration can enhance parameter estimation and improve water table simulations and runoff partitioning.

The advantage obtained from incorporating baseflow calibration in addition to traditional calibration based on measured streamflow alone is demonstrated in this study. A simple lumped unconfined aquifer model developed previously was incorporated into NCAR Community Land Model (CLM) with the SIMTOP runoff parameterization, in which the water table is interactively coupled to the soil moisture through the drainage (groundwater recharge) fluxes. The coupled model (CLMGW) has been successfully validated in Illinois using a unique 22-year (1984–2005) observed monthly data set. In addition, the standard split-sample approach was not applied in this study since the goal of this research was to demonstrate that estimated baseflow can constrain water table depth simulations better than total streamflow. However, as this research moves forward, the split-sample approach will be utilized for model calibration and validation in future applications.

We have conducted sensitivity tests to parameters for different plant type. The major vegetation type in Illinois is corn which has a relatively shallow rooting depth ( $\sim 1.5$  m). Sensitivity tests indicated (not shown here) that if the plant has deeper roots, such as a broadleaf evergreen temperate tree, evapotranspiration increases by about 100 mm/year, whereas total runoff and groundwater level decrease, because deeper roots can extract more water from

deeper soil. When the parameter  $f$  is small, the seasonal cycle of the water table depth is weaker than the case of corn because of extracting more water from the groundwater. Moreover, the parameter  $b$  begins to have an impact on the water table depth and baseflow in the case of temperate-tree during the winter. That is due to the larger leaf area index in the temperate-tree in winter compared to corn. As for the other parameters ( $d_0$  and  $K$ ), no significant difference between the two cases (corn and temperate-tree) can be found.

Due to parameter interactions, various parameter combinations can reproduce the same simulated total runoff, but their flow partitioning and the associated simulations of water table depth as well as other hydrologic variables can be rather different (i.e., equifinality). Using an optimal parameter set identified from baseflow calibration, flow partitioning and water table simulation in land surface models can be improved due to the close dependence of baseflow on water table depth. Observations of soil moisture and water table depth data are extremely difficult to obtain on a regional or global basis; on the other hand, streamflow data is available in many locations. For regions that lack observations of water table depth, baseflow estimates can serve as a surrogate to constrain the water table simulation by land surface models, and help improve storage partitioning between surface runoff and baseflow, as well as soil moisture and groundwater.

Our purpose in this study is to demonstrate that the use of baseflow estimates can constrain water table depth simulations in a land surface model. Although the digital recursive filter lacks a physical basis, it is arguably easy to implement, efficient, reproducible and objective. In addition, only one parameter needs to be specified. In this study, the value of the filter coefficient was carefully chosen based on previous studies which have been compared to either field measurements or traditional hydrograph separation methods. Values of 0.90–0.95 were selected by Nathan and McMahon [44], 0.925 by Arnold et al. [1], 0.971–0.985 by Mugo and Sharma [42], and 0.90–0.95 by Eckhardt [16]. Considering that our ultimate goal is the global implementation of the CLMGW model, the digital filter is perhaps the only approach currently suitable for this purpose. It gives first-order baseflow estimates without being limited by data availability, which is extremely important for global-scale land surface modeling. With the constraints imposed by estimated baseflow, it is believed that large-scale hydrologic simulations can be improved and the commonly encountered equifinality problem in streamflow partitioning can be alleviated in land surface models. Additionally, the development of more robust physically-based digital filters, such as Furey and Gupta [22,23], and their testing and application, deserves future research.

It is worth mentioning that the representativeness of large-scale averaged water table depth such as in this study is an important and difficult issue. Because the important variable in water balance partitioning is storage change in the shallow aquifer, rather than the aquifer storage itself, the near-stream shallow water table areas where storage changes are the largest have more impact on the overall water balance. Hence, the overall aquifer storage changes should be measured near the outlet of the groundwater reservoir, where groundwater discharges into the streams. For the 10 wells in Illinois used in our analysis, which were designed by ISWS to observe the water table response to precipitation, their shallow water table depths as well as their large monthly fluctuations have indicated their close interactions with meteorologic and surface hydrologic processes. Thus they are believed to reflect well the storage changes in the unconfined aquifer system in Illinois. Therefore, it is reasonable to use average water table depth to compare with model results. Moreover, we use the state-average climatic forcing, which we assume will produce a reasonable representation of the average hydrologic response over the entirety of Illinois. In addition, the groundwater scheme used in the CLMGW model accounts

for spatial variability of water table depth by using the statistical-dynamical approach developed by Yeh and Eltahir [64,65].

This study concludes that groundwater parameters in land surface models can be better calibrated from baseflow estimation. However, this approach may be more applicable to shallow water table regions since it is based on the correlation between the groundwater and baseflow. In regions with deep water tables where baseflow may only contribute to a smaller percentage of streamflow, baseflow calibration may not be helpful to constrain model simulations. Furthermore, the optimal parameters estimated in this study are representative for the scale of Illinois: they cannot be necessarily used for different locations, and for varying spatial scales within Illinois. When applying the model to a small watershed, the groundwater rating curve needs to be re-calibrated from local streamflow observations. On the other hand, when applying this modeling framework over large regions, the calibrated parameters need to be calibrated using large-scale flows. Several studies (e.g. [4,61]) showed that calibrated parameters can be regionalized to uncalibrated regions based on climatic and topographic characteristics and streamflow statistics. Our ongoing research includes the implementation of the approach described here for North America and ultimately all the continents.

### Acknowledgement

This research was sponsored by NOAA CPPA Grant NA05OAR4310013. This support is gratefully acknowledged. We would like to express our gratitude to Prof. Zong-Liang Yang and Dr. Guo-Yue Niu for providing the SIMTOP scheme, and Lindsey E. Gulden for discussion. The authors would like to thank Illinois State Water Survey for providing the hydrologic data used here. Computation was supported by Earth System Modeling Facility NSF ATM-0321380.

### References

- [1] Arnold JG, Allen PM, Muttiah R, Bernhardt G. Automated baseflow separation and recession analysis techniques. *Ground Water* 1995;33:1010–8.
- [2] Arnold JG, Allen PM. Validation of automated methods for estimating base flow and groundwater recharge from stream flow records. *J Am Water Resour Assoc* 1999;35(2):411–24.
- [3] Arnold JG, Muttiah RS, Srinivasan R, Allen PM. Regional estimation of baseflow and groundwater recharge in the Upper Mississippi River Basin. *J Hydrol* 2000;227:21–40.
- [4] Bárdossy A. Calibration of hydrological model parameters for ungauged catchments. *Hydrol Earth Syst Sci* 2007;11(2):703–10.
- [5] Beven KJ, Kirkby MJ. A physically based, variable contributing model of basin hydrology. *Hydrol Sci Bull* 1979;24:43–69.
- [6] Beven KJ, Wood EF. Catchment geomorphology and the dynamics of runoff contributing areas. *J Hydrol* 1983;65:139–58.
- [7] Beven KJ. Changing ideas in hydrology—the case of physically-based models. *J Hydrol* 1989;105:157–72.
- [8] Beven KJ, Binley AM. The future of distributed models: model calibration and uncertainty prediction. *Hydrol Process* 1992;6:29–44.
- [9] Bonan GB, Oleson KW, Vertenstein M, Levis S, Zeng X, Dai Y, et al. The land surface climatology of the community land model coupled to the NCAR community climate model. *J Clim* 2002;15:3123–49.
- [10] Bonan GB, Levis S, Kergoat L, Oleson KW. Landscapes as patches of plant functional types: an integrating concept for climate and ecosystem models. *Global Biogeochem Cycles* 2002;16:5.1–5.23.
- [11] Chapman T. Comment on 'Evaluation of automated techniques for baseflow and recession analyses' by R.J. Nathan and T.A. McMahon. *Water Resour Res* 1991;27:1783–4.
- [12] Chen T et al. The project for intercomparison of land-surface parameterization schemes (PILPS) phase 2(c) Cabauw experimental results from the project for intercomparison of land-surface parameterization schemes (PILPS). *J Clim* 1997;10:1194–215.
- [13] Clapp RB, Hornberger GM. Empirical equations for some soil hydraulic properties. *Water Resour Res* 1978;14:601–4.
- [14] Collins WD et al. Description of the NCAR community atmosphere model (CAM 3.0). NCAR Technical Note, Natl Cent for Atmos Res, Boulder, Colo; 2004.
- [15] Duan Q, Sorooshian S, Gupta VK. Effective and efficient global optimization for conceptual rainfall-runoff models. *Water Resour Res* 1992;28:1015–31.
- [16] Eckhardt K. How to construct recursive digital filters for baseflow separation. *Hydrol Process* 2005;19(2):507–15.

- [17] Eltahir EAB, Yeh PJ-F. On the asymmetric response of aquifer water level to floods and droughts in Illinois. *Water Resour Res* 1999;35:1199–217.
- [18] Famiglietti JS, Wood EF. Evapotranspiration and runoff from large land areas—Land surface hydrology for atmospheric general circulation models. *Surv Geophys* 1991;12:179–204.
- [19] Famiglietti JS, Wood EF. Multi-scale modeling of spatially variable water and energy balance processes. *Water Resour Res* 1994;30:3061–78.
- [20] Fan Y, Miguez-Macho G, Weaver C, Walko R, Robock A. Incorporating water table dynamics in climate modeling, part I: water table observations and the equilibrium water table. *J Geophys Res* 2007;112:D10152. doi:10.1029/2006JD008111.
- [21] Fenicia F, Savenije HHG, Matgen P, Pfister L. A comparison of alternative multiobjective calibration strategies for hydrologic modeling. *Water Resour Res* 2007;43:W03434. doi:10.1029/2006WR005098.
- [22] Furey PR, Gupta VK. A physically based filter for separating baseflow from streamflow time series. *Water Resour Res* 2001;37:2709–22.
- [23] Furey PR, Gupta VK. Tests of two physically based filters for base flow separation. *Water Resour Res* 2003;39:1297–307.
- [24] Gallart F, Latron J, Llorens P, Beven KJ. Using internal catchment information to reduce the uncertainty of discharge and baseflow predictions. *Adv Water Resour* 2007;30:808–23.
- [25] Gassman PW, Reyes MR, Green CH, Arnold JG. The soil and water assessment tool: historical development, applications, and future research directions. *Amer Soc Agri Biol Eng* 2007;50:1211–50.
- [26] Gulden LE et al. Improving land-surface model hydrology: is an explicit aquifer model better than a deeper soil profile? *Geophys Res Lett* 2007. doi:10.1029/2007GL029804.
- [27] Güntner A, Uhlenbrook S, Seibert J, Leibundgut C. Multi-criterial validation of TOPMODEL in a mountainous catchment. *Hydrol Process* 1999;13(11):1603–20.
- [28] Gupta HV, Sorooshian S, Yapo PO. Toward improved calibration of hydrologic models: multiple and noncommensurable measures of information. *Water Resour Res* 1998;34:751–63.
- [29] Gusev YM, Nasonova ON. The simulation of heat and water exchange at the land-atmosphere interface for boreal grassland by the land-surface model SWAP. *Hydrol Process* 2002;16:1893–919.
- [30] Gutowski WJ et al. A coupled land-atmosphere simulation progress (CLASP): calibration and validation. *J Geophys Res* 2002;107:4283. doi:10.1029/2001JD000392.
- [31] Hollinger SE, Isard SA. A soil moisture climatology of Illinois. *J Clim* 1994;7:822–33.
- [32] Houser PR, Gupta HV, Shuttleworth WJ, Famiglietti JS. Multiobjective calibration and sensitivity of a distributed land surface water and energy balance model. *J Geophys Res* 2001;106:33,42133421–3333433.
- [33] Kanamitsu M, Ebisuzaki W, Woollen J, Yang S-K, Hnilo JJ, Fiorino M, et al. NCEP-DOE AMIP-II Reanalysis (R-2). *Bull Amer Meteor Soc* 2002;83:1631–43.
- [34] Koster RD, Suarez MJ, Ducharme A, Stieglitz M, Kumar P. A catchment-based approach to modeling land surface processes in a general circulation model: 1. Model structure. *J Geophys Res* 2000;105:24,80924809–2224822.
- [35] Liang X, Xie Z. A new surface runoff parameterization with subgrid-scale soil heterogeneity for land surface models. *Adv Water Resour* 2001;24:1173–93.
- [36] Liang X, Xie Z, Huang M. A new parameterization for surface and groundwater interactions and its impact on water budgets with the variable infiltration capacity (VIC) land surface model. *J Geophys Res* 2003;108:8613. doi:10.1029/2002JD003090.
- [37] Lim KJ et al. Automated web GIS based hydrograph analysis tool, WHAT. *J Am Water Resour Assoc* 2005;41:1407–16.
- [38] Lyne V, Hollick M. Stochastic time-variable rainfall-runoff modeling. *Natl Conf Publ Inst Eng Aust* 1979;79:89–92.
- [39] Mau DP, Winter TC. Estimating ground-water recharge and baseflow from streamflow hydrographs for a small watershed in New Hampshire. *Ground Water* 1997;35:291–304.
- [40] Maxwell RM, Miller NL. Development of a coupled land surface and groundwater model. *J Hydrometeorol* 2005;6:233–47.
- [41] Miguez-Macho G, Fan Y, Weaver CP, Walko R, Robock A. Incorporating water table dynamics in climate modeling: 2. Formulation, validation, and soil moisture simulation. *J Geophys Res* 2007;112:D13108. doi:10.1029/2006JD008112.
- [42] Mugo JM, Sharma TC. Application of a conceptual method for separating runoff components in daily hydrographs in Kimakia Forest catchments, Kenya. *Hydrol Process* 1999;13:2931–9.
- [43] Nash JE, Sutcliffe JV. River flow forecasting through conceptual models part I—a discussion of principles. *J Hydrol* 1970;10:282–90.
- [44] Nathan RJ, McMahon TA. Evaluation of automated techniques for baseflow and recession analysis. *Water Resour Res* 1990;26:1465–73.
- [45] Niu G-Y, Yang Z-L, Dickinson RE, Gulden LE. A simple TOPMODEL-based runoff parameterization (SIMTOP) for use in global climate models. *J Geophys Res* 2005;110:D21106. doi:10.1029/2005JD006111.
- [46] Niu G-Y, Yang Z-L. Effects of frozen soil on snowmelt runoff and soil water storage at a continental scale. *J Hydrometeorol* 2006;7:937–52.
- [47] Niu G-Y, Yang Z-L, Dickinson RE, Gulden LE, Su H. Development of a simple groundwater model for use in climate models and evaluation with gravity recovery and climate experiment data. *J Geophys Res* 2007;112:D07103. doi:10.1029/2006JD007522.
- [48] Oleson KW et al. Technical description of the community land model (CLM). Technical Note NCAR/TN-461+STR, Natl Cent for Atmos Res, Boulder, Colo; 2004. p. 174.
- [49] Quinn PF, Beven KJ. Spatial and temporal predictions of soil moisture dynamics, runoff variable source areas and evapotranspiration for Plynlimon, mid-Wales. *Hydrol Process* 1993;7:425–48.
- [50] Shao Y, Henderson-Sellers A. Validation of soil moisture simulation in landsurface parameterization schemes with HAPEX data. *Global Planet Change* 1996;13:11–46.
- [51] Singh VP. *Elem Hydrol* 1992:302–24.
- [52] Son K, Sivapalan M. Improving model structure and reducing parameter uncertainty in conceptual water balance models through the use of auxiliary data. *Water Resour Res* 2007;43:W01415. doi:10.1029/2006WR005032.
- [53] Sorooshian S, Gupta VK. Automatic calibration of conceptual rainfall-runoff models: the question of parameter observability and uniqueness. *Water Resour Res* 1983;19:260–8.
- [54] Sorooshian S, Duan Q, Gupta VK. Calibration of rainfall-runoff models: application of global optimization to the sacramento soil moisture accounting model. *Water Resour Res* 1993;29:1185–94.
- [55] Spongberg ME. Spectral analysis of base flow separation with digital filters. *Water Resour Res* 2000;36:745–52.
- [56] Srinivasan R, Arnold JG. Integration of basin-scale water quality model with GIS. *Water Resour Bull* 1994;30:453–62.
- [57] Stieglitz M, Rind D, Famiglietti JS, Rosenzweig C. An efficient approach to modeling the topographic control of surface hydrology for regional and global modeling. *J Clim* 1997;10:118–37.
- [58] Szilagyi J, Parlange MB, Albertson JD. Recession flow analysis for aquifer parameter determination. *Water Resour Res* 1998;34(7):1851–7.
- [59] Szilagyi J. Heuristic continuous base flow separation. *J Hydrol Eng* 2004;9(4):311–8.
- [60] Wood EF et al. The project for intercomparison of land-surface parameterization schemes (PILPS) phase 2(c) Red-Arkansas River basin experiment: 1. Experiment description and summary intercomparison. *Global Planet Change* 1998;19:115–35.
- [61] Xie Z, Yuan F, Duan Q, Zheng J, Liang M, Chen F. Regional parameter estimation of the VIC land surface model: methodology and application to river basins in China. *J Hydrometeorol* 2007;8(3):447–68.
- [62] Yapo PO, Gupta HV, Sorooshian S. Multi-objective global optimization for hydrologic models. *J Hydrol* 1998;204:83–97.
- [63] Yeh PJ-F, Irizarry M, Eltahir EAB. Hydroclimatology of Illinois: a comparison of monthly evaporation estimates based on atmospheric water balance and soil water balance. *J Geophys Res* 1998;103:19,82319823–3719837.
- [64] Yeh PJ-F, Eltahir EAB. Representation of water table dynamics in a land surface scheme. Part I: Model development. *J Clim* 2005;18:1861–80.
- [65] Yeh PJ-F, Eltahir EAB. Representation of water table dynamics in a land surface scheme. Part II: Subgrid variability. *J Clim* 2005;18:1881–901.
- [66] Yeh PJ-F, Famiglietti JS. Regional groundwater evapotranspiration in Illinois, *J Hydrometeorol*, submitted for publication.
- [67] York JP, Person M, Gutowski WJ, Winter TC. Putting aquifers into atmospheric simulation models: an example from the Mill Creek Watershed, northeastern Kansas. *Adv Water Resour* 2002;25:221–38.
- [68] Yu Z, Schwartz FW. Automated calibration applied to watershed-scale flow simulations. *Hydrol Process* 1999;13:191–209.
- [69] Zeng X. Global vegetation root distribution for land modeling. *J Hydrometeorol* 2001;2:525–30.